

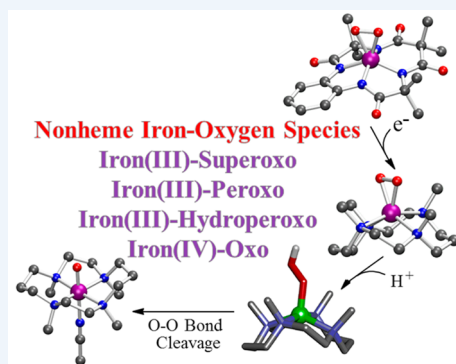
# Synthetic Mononuclear Nonheme Iron–Oxygen Intermediates

Published as part of the Accounts of Chemical Research special issue “Synthesis in Biological Inorganic Chemistry”.

Wonwoo Nam\*

Department of Chemistry and Nano Science, Ewha Womans University, Seoul 120-750, Korea

**CONSPECTUS:** Mononuclear nonheme iron–oxygen species, such as iron–superoxo, –peroxo, –hydroperoxo, and –oxo, are key intermediates involved in dioxygen activation and oxidation reactions catalyzed by nonheme iron enzymes. Because these iron–oxygen intermediates are short-lived due to their thermal instability and high reactivity, it is challenging to investigate their structural and spectroscopic properties and reactivity in the catalytic cycles of the enzymatic reactions themselves. One way to approach such problems is to synthesize biomimetic iron–oxygen complexes and to tune their geometric and electronic structures for structural characterization and reactivity studies. Indeed, a number of biologically important iron–oxygen species, such as mononuclear nonheme iron(III)–superoxo, iron(III)–peroxo, iron(III)–hydroperoxo, iron(IV)–oxo, and iron(V)–oxo complexes, were synthesized recently, and the first X-ray crystal structures of iron(III)–superoxo, iron(III)–peroxo, and iron(IV)–oxo complexes in nonheme iron models were successfully obtained. Thus, our understanding of iron–oxygen intermediates in biological reactions has been aided greatly from the studies of the structural and spectroscopic properties and the reactivities of the synthetic biomimetic analogues.



In this Account, we describe our recent results on the synthesis and characterization of mononuclear nonheme iron–oxygen complexes bearing simple macrocyclic ligands, such as *N*-tetramethylated cyclam ligand (TMC) and tetraamido macrocyclic ligand (TAML). In the case of iron–superoxo complexes, an iron(III)–superoxo complex, [(TAML)Fe<sup>III</sup>(O<sub>2</sub>)]<sup>2-</sup>, is described, including its crystal structure and reactivities in electrophilic and nucleophilic oxidative reactions, and its properties are compared with those of a chromium(III)–superoxo complex, [(TMC)Cr<sup>III</sup>(O<sub>2</sub>)(Cl)]<sup>+</sup>, with respect to its reactivities in hydrogen atom transfer (HAT) and oxygen atom transfer (OAT) reactions. In the case of iron–peroxo intermediates, an X-ray crystal structure of an iron(III)–peroxo complex binding the peroxo ligand in a side-on ( $\eta^2$ ) fashion, [(TMC)Fe<sup>III</sup>(O<sub>2</sub>)]<sup>+</sup>, is described. In addition, iron(III)–peroxo complexes binding redox-inactive metal ions are described and discussed in light of the role of redox-inactive metal ions in O–O bond activation in cytochrome *c* oxidase and O<sub>2</sub>-evolution in photosystem II. In the case of iron–hydroperoxo intermediates, mononuclear nonheme iron(III)–hydroperoxo complexes can be generated upon protonation of iron(III)–peroxo complexes or by hydrogen atom abstraction (HAA) of hydrocarbon C–H bonds by iron(III)–superoxo complexes. Reactivities of the iron(III)–hydroperoxo complexes in both electrophilic and nucleophilic oxidative reactions are described along with a discussion of O–O bond cleavage mechanisms. In the last section of this Account, a brief summary is presented of developments in mononuclear nonheme iron(IV)–oxo complexes since the first structurally characterized iron(IV)–oxo complex, [(TMC)Fe<sup>IV</sup>(O)]<sup>2+</sup>, was reported. Although the field of nonheme iron–oxygen intermediates (e.g., Fe–O<sub>2</sub>, Fe–O<sub>2</sub>H, and Fe–O) has been developed greatly through intense synthetic, structural, spectroscopic, reactivity, and theoretical studies in the communities of bioinorganic and biomimetic chemistry over the past 10 years, there is still much to be explored in trapping, characterizing, and understanding the chemical properties of the key iron–oxygen intermediates involved in dioxygen activation and oxidation reactions by nonheme iron enzymes and their biomimetic compounds.

## INTRODUCTION

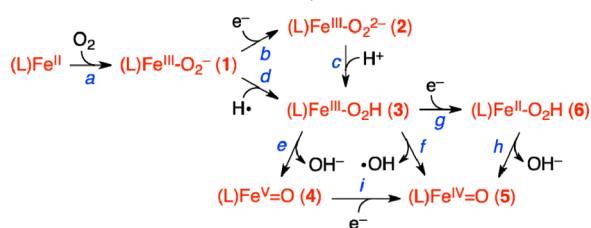
Dioxygen (O<sub>2</sub>) is utilized in a variety of biological reactions mediated by metalloenzymes. These enzymes use diverse active sites, such as heme and nonheme iron, copper, and other metal sites, to carry out a broad range of oxidative reactions by activating dioxygen, such as epoxidation, hydroxylation, halogenation, *cis*-dihydroxylation, and *N*-dealkylation.<sup>1</sup> Despite the diversity of the active sites, only a few key metal–oxygen intermediates, including metal–superoxo, –peroxo, –hydroperoxo, and –oxo species, are involved in the dioxygen activation and oxidation reactions by the metalloenzymes.<sup>1–7</sup>

For example, some heme and mononuclear nonheme iron enzymes utilize high-spin iron(II) ions at their active sites to bind O<sub>2</sub>, thereby generating iron(III)–superoxo species (1) (Scheme 1, reaction a). The iron(III)–superoxo species are then converted to the corresponding iron(III)–peroxo species (2) by one-electron reduction (Scheme 1, reaction b), followed by conversion of the resulting iron(III)–peroxo species to an iron(III)–hydroperoxo species (3) upon protonation (Scheme

Received: April 18, 2015

Published: July 23, 2015

**Scheme 1. Unified Mechanisms for Dioxygen Activation by Heme and Nonheme Iron Enzymes**



1, reaction c). Alternatively, the iron(III)–hydroperoxo species can be generated directly from the iron(III)–superoxo species by abstracting one hydrogen atom from substrates (Scheme 1, reaction d).<sup>3</sup> The latter reaction has been found to occur in nonheme iron enzymes but not in heme enzymes. Finally, the heterolytic O–O bond cleavage of the iron(III)–hydroperoxo species affords high-valent iron(V)–oxo species (4) (or iron(IV)–oxo porphyrin  $\pi$ -cation radical in heme systems)<sup>8</sup> (Scheme 1, reaction e), whereas high-valent iron(IV)–oxo species (5) are formed via O–O bond homolysis of the iron(III)–hydroperoxo species (Scheme 1, reaction f). In nonheme iron enzymes, high-valent iron(IV)–oxo species are also formed through one-electron reduction of the iron(III)–hydroperoxo species to the corresponding iron(II)–hydroperoxo species (6) (Scheme 1, reaction g), followed by a subsequent heterolytic O–O bond cleavage of the latter species (Scheme 1, reaction h).<sup>3,9,10</sup>

Our understanding of the iron–oxygen intermediates in dioxygen activation reactions catalyzed by heme and nonheme iron enzymes has been aided significantly by the studies of the structural and spectroscopic properties and reactivities of their biomimetic compounds. Indeed, a number of biologically relevant iron–oxygen complexes have been synthesized recently in nonheme iron model studies, such as mononuclear nonheme iron(III)–superoxo, iron(III)–peroxo, iron(III)–hydroperoxo, iron(IV)–oxo, and iron(V)–oxo complexes bearing simple macrocyclic ligands.<sup>11–15</sup> One notable example is the first structurally characterized mononuclear nonheme iron(IV)–oxo complex bearing an *N*-tetramethylated cyclam ligand, [(14-TMC)Fe<sup>IV</sup>(O)]<sup>2+</sup> (14-TMC, 1,4,8,11-tetramethyl-1,4,8,11-tetraazacyclotetradecane) (Figure 1a).<sup>16</sup> The success of the isolation and full characterization of the nonheme iron(IV)–oxo complex opened a new area in the biomimetic studies of nonheme iron enzymes. Since then, a number of nonheme iron(IV)–oxo complexes have been synthesized and investigated to elucidate the structural and chemical properties of biologically important iron(IV)–oxo intermediates.<sup>11–13,15,17–19</sup> Another important synthetic iron–oxygen intermediate reported with its X-ray crystal structure was the mononuclear nonheme iron(III)–peroxo complex bearing the 14-TMC ligand, [(14-TMC)Fe<sup>III</sup>(O<sub>2</sub>)]<sup>+</sup> (Figure 1b).<sup>20</sup> In this study, a clean conversion of the nonheme iron(III)–peroxo complex to the corresponding iron(III)–hydroperoxo and iron(IV)–oxo complexes was also demonstrated, and reactivities of the isolated iron(III)–peroxo, iron(III)–hydroperoxo, and iron(IV)–oxo complexes were compared directly in electrophilic and nucleophilic oxidative reactions.<sup>20</sup> Very recently, a crystal structure of a mononuclear nonheme iron(III)–superoxo complex bearing a tetraamido macrocyclic ligand (TAML), [(TAML)Fe<sup>III</sup>(O<sub>2</sub>)]<sup>2-</sup> (Figure 1c), was successfully obtained with full spectroscopic characterization.<sup>21</sup> Interestingly, the isolated nonheme iron(III)–superoxo com-

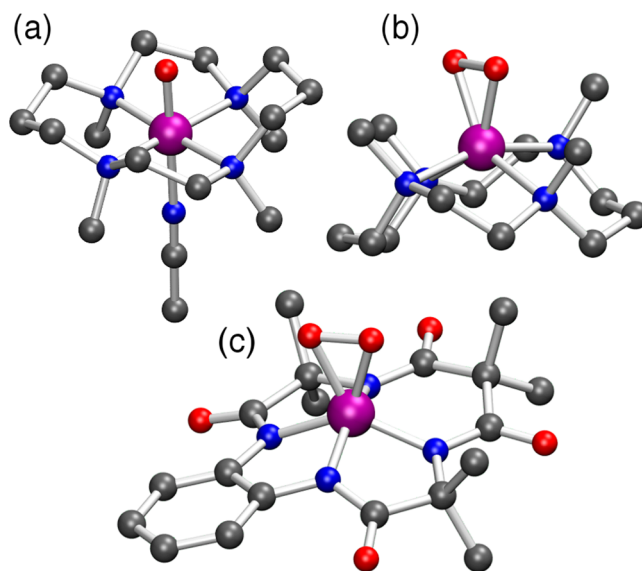


**Figure 1.** Crystal structures of mononuclear nonheme iron(IV)–oxo, [(14-TMC)Fe<sup>IV</sup>(O)]<sup>2+</sup> (a),<sup>16</sup> iron(III)–peroxo, [(14-TMC)Fe<sup>III</sup>(O<sub>2</sub>)]<sup>+</sup> (b),<sup>20</sup> and iron(III)–superoxo, [(TAML)Fe<sup>III</sup>(O<sub>2</sub>)]<sup>2-</sup> (c),<sup>21</sup> complexes. Atom colors: purple = Fe, dark gray = C, blue = N, red = O.

plex showed reactivities in both electrophilic and nucleophilic oxidative reactions. As evidenced by the three crystal structures of the synthetic mononuclear nonheme iron–oxygen complexes reported recently, we have observed striking advances for the past 10 years in the structural and spectroscopic characterization of the biomimetic mononuclear nonheme iron–oxygen intermediates and their chemical properties in oxidation reactions. In this Account, we summarize our recent results on the synthesis, spectroscopic and structural characterization, and reactivity studies of the biomimetic compounds of mononuclear nonheme iron–oxygen intermediates involved in enzymatic reactions.

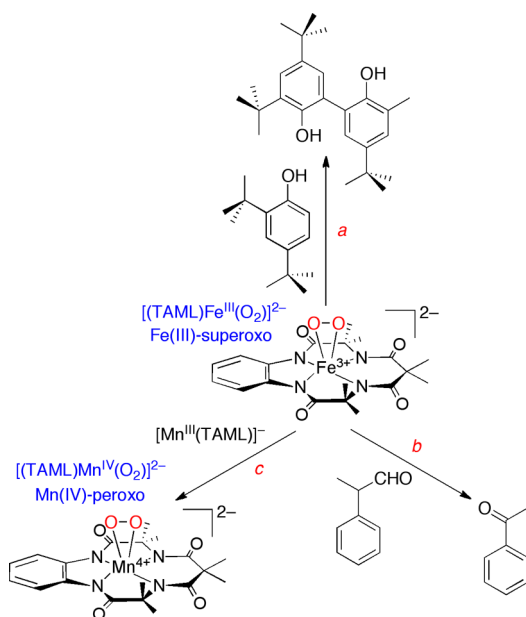
## ■ MONONUCLEAR NONHEME IRON(III)–SUPEROXO COMPLEXES

The first step in dioxygen activation at an iron(II) center is the binding of O<sub>2</sub>, thereby generating an iron(III)–superoxo species (1) (Scheme 1, reaction a). The iron(III)–superoxo species have attracted much attention recently in the communities of biological and bioinorganic chemistry, as they have been invoked as active oxidants in the C–H bond activation and oxygen atom transfer (OAT) reactions in nonheme iron enzymes.<sup>3,22</sup> Although iron(III)–superoxo species in heme systems were well characterized including crystal structures in the 1970s,<sup>23,24</sup> there are only a couple of synthetic nonheme iron(III)–superoxo complexes reported very recently. Those are the structurally and spectroscopically characterized side-on ( $\eta^2$ ) iron(III)–superoxo complex, [(TAML)Fe<sup>III</sup>(O<sub>2</sub>)]<sup>2-</sup> (Figure 1c),<sup>21</sup> and the spectroscopically characterized iron(III)–superoxo complex, (BDPP)Fe<sup>III</sup>(O<sub>2</sub>) (H<sub>2</sub>BDPP, 2,6-bis(((*S*)-2-(diphenylhydroxymethyl)-1-pyrrolidinyl)methyl)pyridine).<sup>25</sup>

The [(TAML)Fe<sup>III</sup>(O<sub>2</sub>)]<sup>2-</sup> complex was synthesized by reacting Na[Fe<sup>III</sup>(TAML)] with KO<sub>2</sub> in the presence of 2,2,2-cryptand in CH<sub>3</sub>CN at 5 °C,<sup>21</sup> whereas the [(BDPP)Fe<sup>III</sup>(O<sub>2</sub>)] complex was synthesized by bubbling O<sub>2</sub> into the THF solution of Fe<sup>II</sup>(BDPP) at –80 °C.<sup>25</sup> Due to the high thermal stability of

$[(\text{TAML})\text{Fe}^{\text{III}}(\text{O}_2)]^{2-}$ , this iron(III)–superoxo complex could be characterized with various spectroscopic techniques, such as UV–vis, infrared, Mössbauer, electrospray ionization mass (ESI-MS), and electron paramagnetic resonance (EPR) spectroscopies, and X-ray crystallography for structure.<sup>21</sup> In the crystal structure of  $[(\text{TAML})\text{Fe}^{\text{III}}(\text{O}_2)]^{2-}$  (Figure 1c), the  $\text{O}_2$ -unit is bound to an iron ion in a side-on ( $\eta^2$ ) fashion with the O–O bond length of  $\sim 1.32$  Å, which is similar to those of Fe(II)–superoxo species found in homoprotocatechuate 2,3-dioxygenase (1.34 Å)<sup>26</sup> and other metal–superoxo complexes (1.2–1.3 Å).<sup>27</sup> The superoxo character of the  $\text{O}_2$  ligand was further supported by the infrared spectrum taken in  $\text{CH}_3\text{CN}$  at  $-40$  °C, exhibiting an isotopically sensitive band at  $1260$   $\text{cm}^{-1}$ , which shifts to  $1183$   $\text{cm}^{-1}$  upon substitution of  $^{16}\text{O}$  with  $^{18}\text{O}$ .<sup>21</sup> In reactivity studies, the  $[(\text{TAML})\text{Fe}^{\text{III}}(\text{O}_2)]^{2-}$  complex showed reactivities in both electrophilic and nucleophilic oxidation reactions. In the oxidation of *para*-substituted 2,6-di-*tert*-butylphenols (*para*-*X*-2,6-*tert*- $\text{Bu}_2\text{-C}_6\text{H}_2\text{OH}$ ) (Scheme 2,

**Scheme 2.**  $[(\text{TAML})\text{Fe}^{\text{III}}(\text{O}_2)]^{2-}$  in Oxidation and  $\text{O}_2$ -Transfer Reactions



reaction a), we have observed a good correlation between reaction rates and O–H bond dissociation energies (BDE) of *para*-*X*-2,6-*tert*- $\text{Bu}_2\text{-C}_6\text{H}_2\text{OH}$ , demonstrating that the superoxo ligand in  $[(\text{TAML})\text{Fe}^{\text{III}}(\text{O}_2)]^{2-}$  possesses an electrophilic character enabling O–H bond activation reactions. Interestingly, the  $[(\text{TAML})\text{Fe}^{\text{III}}(\text{O}_2)]^{2-}$  complex also showed reactivity in the oxidation of aldehydes such as 2-phenylpropionaldehyde and *para*-substituted benzaldehydes (*para*-*X*-benzaldehydes) (Scheme 2, reaction b); a positive Hammett  $\rho$  value of 1.4 suggests a nucleophilic reactivity for the iron(III)–superoxo complex. It is worth noting here that the nucleophilic reactivity of a copper(II)–superoxo complex was reported recently.<sup>28</sup> Another interesting reactivity of the  $[(\text{TAML})\text{Fe}^{\text{III}}(\text{O}_2)]^{2-}$  complex was an intermolecular  $\text{O}_2$ -transfer from  $[(\text{TAML})\text{Fe}^{\text{III}}(\text{O}_2)]^{2-}$  to  $[\text{Mn}^{\text{II}}(\text{TAML})]^-$ , resulting in the formation of  $[\text{Fe}^{\text{III}}(\text{TAML})]^-$  and  $[(\text{TAML})\text{Mn}^{\text{IV}}(\text{O}_2)]^{2-}$  (Scheme 2, reaction c). The X-ray crystal structure of the Mn(IV)–peroxo product,  $[(\text{TAML})\text{Mn}^{\text{IV}}(\text{O}_2)]^{2-}$ , clearly showed the binding of

the  $\text{O}_2$ -unit in a side-on ( $\eta^2$ ) fashion with an O–O bond length of  $\sim 1.41$  Å.<sup>21</sup>

Compared with the  $[(\text{TAML})\text{Fe}^{\text{III}}(\text{O}_2)]^{2-}$  complex,  $(\text{BDPP})\text{Fe}^{\text{III}}(\text{O}_2)$  was generated at a low temperature, probably, due to a lesser thermal stability.<sup>25</sup> Although no structural information, such as the binding mode of the superoxo ligand (e.g., side-on versus end-on), was reported, all the spectroscopic data, including resonance Raman (rRaman; for example, an isotopically sensitive band at  $1125$   $\text{cm}^{-1}$ ), Mössbauer, and EPR spectroscopies, supported the binding of a superoxo ligand to an iron(III) ion. This iron(III)–superoxo complex showed reactivity in hydrogen atom abstraction (HAA) reactions for substrates with weak C–H bonds; the reaction of  $(\text{BDPP})\text{Fe}^{\text{III}}(\text{O}_2)$  with 9,10-dihydroanthracene (DHA) at  $-70$  °C afforded anthracene as the sole product with a kinetic isotope effect (KIE) value of 7.<sup>25</sup>

Other synthetic metal–superoxo complexes with first-row transition metals (e.g., from Cr to Cu) have been used in the studies of structural and chemical properties and reactivities in various oxidation reactions.<sup>6,14,29,30</sup> For example, an end-on chromium(III)–superoxo complex bearing the 14-TMC ligand,  $[(14\text{-TMC})\text{Cr}^{\text{III}}(\text{O}_2)(\text{Cl})]^+$ , was reported with structural and spectroscopic characterization and reactivities in HAA and oxygen atom transfer (OAT) reactions.<sup>31,32</sup> The X-ray crystal structure of the Cr(III)–superoxo complex clearly showed binding of the  $\text{O}_2$ -unit in an end-on ( $\eta^1$ ) fashion with an O–O bond length of 1.231 Å; the  $\text{O}_2$ -unit is pointed away from the four *N*-methyl groups of the 14-TMC ligand (Figure 2a). In

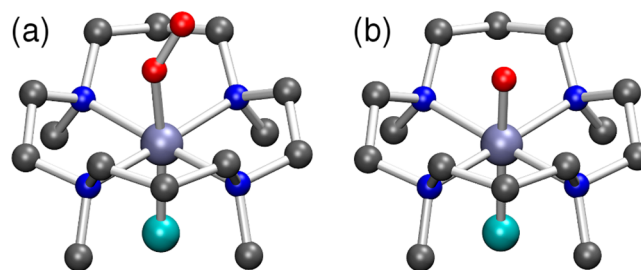
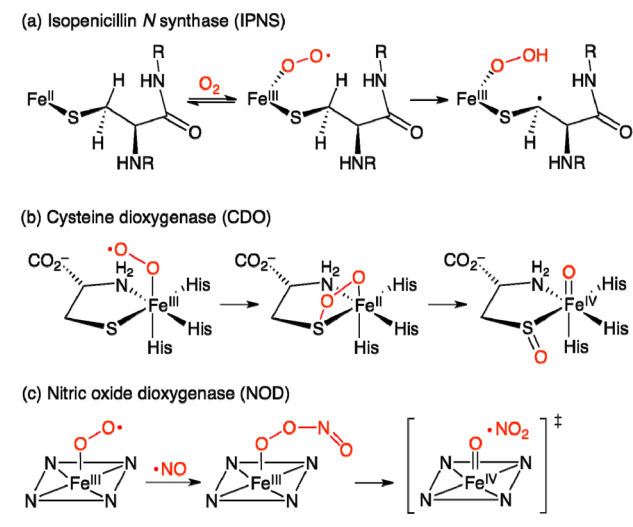


**Figure 2.** Crystal structures of mononuclear nonheme Cr(III)–superoxo,  $[(14\text{-TMC})\text{Cr}^{\text{III}}(\text{O}_2)(\text{Cl})]^+$  (a), and Cr(IV)–oxo,  $[(14\text{-TMC})\text{Cr}^{\text{IV}}(\text{O})(\text{Cl})]^+$  (b), complexes.<sup>31</sup> Atom colors: light purple = Cr, dark gray = C, blue = N, red = O, green = Cl.

addition, the O–O bond stretching vibration of  $[(14\text{-TMC})\text{Cr}^{\text{III}}(^{16}\text{O}_2)(\text{Cl})]^+$ , determined by rRaman spectroscopy in  $\text{CH}_3\text{CN}$  at  $-20$  °C, appeared at  $1170$   $\text{cm}^{-1}$ , which shifts to  $1104$   $\text{cm}^{-1}$  in  $[(14\text{-TMC})\text{Cr}^{\text{III}}(^{18}\text{O}_2)(\text{Cl})]^+$ . This isolated Cr(III)–superoxo complex was used in the kinetic studies of HAA and OAT reactions with external substrates.<sup>31,32</sup> In the HAA reactions, the observations of the dependence of the rate constants on the C–H BDE of hydrocarbons and a high KIE value of  $\sim 50$  in the oxidation of DHA and DHA- $d_4$  indicate that the H atom abstraction by the Cr(III)–superoxo complex is the rate-determining step; this study provided strong evidence demonstrating that metal–superoxo species are capable of abstracting a H-atom from substrate C–H bonds, as proposed in the nonheme iron(III)–superoxo species in isopenicillin *N* synthase (IPNS) (see Scheme 3a, IPNS).<sup>3,22</sup> In the oxidation of phosphine and sulfides (i.e., OAT reactions), the distal oxygen of the superoxo ligand was transferred to the substrate to give an oxygenated product, whereas the proximal oxygen remained bound to the Cr<sup>IV</sup> ion to give  $[(14\text{-$

### Scheme 3. Iron(III)–Superoxo Species in Hydrogen Atom Abstraction (a), Oxygen Atom Transfer (b), and NO (c) Reactions



TMC)Cr<sup>IV</sup>(O)(Cl)]<sup>+</sup> as a product. The X-ray crystal structure of the Cr(IV)–oxo complex shows that each of the four *N*-methyl groups point away from the Cr–oxo moiety, as observed in the structure of [(14-TMC)Fe<sup>IV</sup>(O)]<sup>2+</sup>,<sup>16</sup> with the Cr–O bond length of 1.698 Å (Figure 2b). The rRaman spectrum of the Cr(IV)–oxo complex, [(14-TMC)Cr<sup>IV</sup>(O)(Cl)]<sup>+</sup>, exhibits an isotopically sensitive band at 874 cm<sup>−1</sup>, which is higher than the Fe–O frequency of [(14-TMC)Fe<sup>IV</sup>(O)(NCCH<sub>3</sub>)]<sup>2+</sup> (834 cm<sup>−1</sup>).<sup>33</sup> The observations of the metal–superoxo complex involvement in sulfoxidation and the formation of a metal–oxo species as a product in the sulfoxidation reaction support the proposed oxidant and mechanism in the cysteine dioxygenase (CDO) reactions; an iron(III)–superoxo species is an active oxidant that attacks the sulfur atom of the cysteine ligand by the terminal oxygen atom of the superoxo group, resulting in the formation of a sulfonate and an iron(IV)–oxo species (see Scheme 3b, CDO).<sup>22</sup> The electrophilic character of the superoxo ligand in [(14-TMC)Cr<sup>III</sup>(O<sub>2</sub>)(Cl)]<sup>+</sup> was demonstrated unambiguously in the sulfoxidation of *para*-substituted thioanisoles (*para*-X-thioanisoles) with a Hammett  $\rho$  value of  $-3.3$ .<sup>32</sup> Finally, the [(14-TMC)Cr<sup>III</sup>(O<sub>2</sub>)(Cl)]<sup>+</sup> complex was used as a biomimetic compound of nitric oxide dioxygenases (NODs) (see Scheme 3c, NOD); the reaction of [(14-TMC)Cr<sup>III</sup>(O<sub>2</sub>)(Cl)]<sup>+</sup> and nitric oxide (NO) generated [(14-TMC)Cr<sup>IV</sup>(O)(Cl)]<sup>+</sup> via a

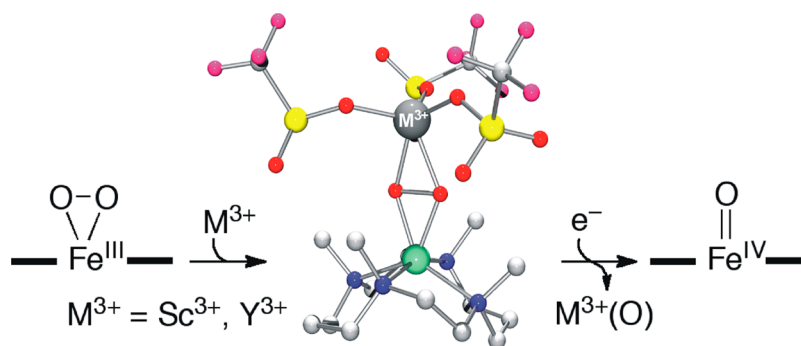
presumed Cr(III)–peroxynitrite intermediate, [(14-TMC)Cr<sup>III</sup>(OON=O)(Cl)]<sup>+</sup>.<sup>34</sup>

### MONONUCLEAR NONHEME IRON(III)–PEROXO COMPLEXES

Iron(III)–peroxo species (2) are formed upon one electron reduction of iron(III)–superoxo species (Scheme 1, reaction b). Although the chemistry of the iron(III)–peroxo species has been well developed in biomimetic heme systems,<sup>35</sup> it was in nonheme iron systems that the first high-resolution crystal structure of a synthetic iron(III)–peroxo complex was successfully obtained (Figure 1b).<sup>20</sup> The X-ray crystal structure of the [(14-TMC)Fe<sup>III</sup>(O<sub>2</sub>)]<sup>+</sup> complex exhibits the binding of a peroxo ligand in a side-on ( $\eta^2$ ) fashion with an O–O bond length of 1.463 Å; the Fe–O<sub>2</sub> geometry is similar to the crystallographically characterized structure of naphthalene dioxygenases (NDO), where the O<sub>2</sub>-unit binds to the mononuclear iron center in a side-on ( $\eta^2$ ) fashion with an O–O bond length of 1.45 Å.<sup>36</sup> In the structure, all four *N*-methyl groups point to the same side of the Fe–O<sub>2</sub> moiety, which is different from the Cr(III)–superoxo complex, [(14-TMC)Cr<sup>III</sup>(O<sub>2</sub>)(Cl)]<sup>+</sup>,<sup>31</sup> but similar to other metal–peroxo complexes bearing TMC ligands, such as [(12-TMC)Cr<sup>IV</sup>(O<sub>2</sub>)(Cl)]<sup>+</sup>,<sup>37</sup> [(12-TMC)Mn<sup>III</sup>(O<sub>2</sub>)]<sup>+</sup>,<sup>38</sup> [(13-TMC)Mn<sup>III</sup>(O<sub>2</sub>)]<sup>+</sup>,<sup>14</sup> [(14-TMC)Mn<sup>III</sup>(O<sub>2</sub>)]<sup>+</sup>,<sup>14</sup> [(12-TMC)Co<sup>III</sup>(O<sub>2</sub>)]<sup>+</sup>,<sup>14</sup> [(13-TMC)Co<sup>III</sup>(O<sub>2</sub>)]<sup>+</sup>,<sup>14</sup> [(12-TMC)Ni<sup>III</sup>(O<sub>2</sub>)]<sup>+</sup>,<sup>14</sup> and [(13-TMC)Ni<sup>III</sup>(O<sub>2</sub>)]<sup>+</sup>.<sup>39</sup> Reactivities of the metal–peroxo complexes, including the iron(III)–peroxo complex, were well demonstrated in nucleophilic oxidation reactions.<sup>6,14,38,39</sup>

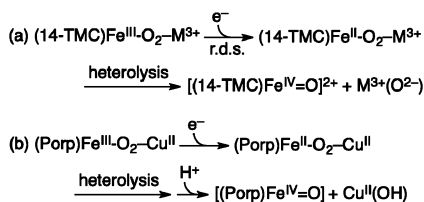
Very recently, binding of redox-inactive metal ions to a mononuclear nonheme iron(III)–peroxo complex was reported in the reaction of [(14-TMC)Fe<sup>III</sup>(O<sub>2</sub>)]<sup>+</sup> with scandium triflate, Sc(CF<sub>3</sub>SO<sub>3</sub>)<sub>3</sub>, and yttrium triflate, Y(CF<sub>3</sub>SO<sub>3</sub>)<sub>3</sub> (Scheme 4).<sup>40,41</sup> Based on the characterization with various spectroscopic methods, such as UV–vis, EPR, rRaman, ESI-MS, and XAS/EXAFS, the intermediates were assigned as mononuclear iron(III)–peroxo complexes binding a peroxo ligand in a side-on ( $\eta^2$ ) fashion between two metal ions, (14-TMC)Fe<sup>III</sup>–( $\mu, \eta^2: \eta^2$ -O<sub>2</sub>)–M<sup>3+</sup> (M<sup>3+</sup> = Sc<sup>3+</sup> and Y<sup>3+</sup>) (Scheme 4). The fundamental electron-transfer properties of the (14-TMC)Fe<sup>III</sup>–(O<sub>2</sub>)–M<sup>3+</sup> complexes, such as one-electron reduction potentials ( $E_{\text{red}}$ ) and reorganization energies in electron transfer ( $\lambda$ ), were then investigated by carrying out electron-transfer reactions with electron donors (e.g., ferrocene (Fc) and its derivatives); the  $E_{\text{red}}$  values of (14-TMC)Fe<sup>III</sup>–(O<sub>2</sub>)–Sc<sup>3+</sup> and (14-TMC)Fe<sup>III</sup>–(O<sub>2</sub>)–Y<sup>3+</sup> were estimated to be 0.40 and 0.16 V vs SCE, respectively, and the  $\lambda$  values were evaluated to be 1.29 eV for both complexes.<sup>40</sup> Further, it was

### Scheme 4. Synthesis of (14-TMC)Fe<sup>III</sup>–(O<sub>2</sub>)–M<sup>3+</sup> and Its One-Electron Reduction Reaction



shown that the reaction of  $(14\text{-TMC})\text{Fe}^{\text{III}}-(\text{O}_2)-\text{M}^{3+}$  with electron donors afforded formation of  $[(14\text{-TMC})\text{Fe}^{\text{IV}}(\text{O})]^{2+}$  (Scheme 4).<sup>40</sup> In this reaction, the conversion rates of  $(14\text{-TMC})\text{Fe}^{\text{III}}-(\text{O}_2)-\text{M}^{3+}$  to  $[(14\text{-TMC})\text{Fe}^{\text{IV}}(\text{O})]^{2+}$  were dependent on the Lewis acidity of the redox-inactive metal ions and the oxidation potential of the electron donors. A mechanism for the reactions of  $(14\text{-TMC})\text{Fe}^{\text{III}}-(\text{O}_2)-\text{M}^{3+}$  and electron donors was proposed as follows:  $(14\text{-TMC})\text{Fe}^{\text{III}}-(\text{O}_2)-\text{M}^{3+}$  is reduced to  $(14\text{-TMC})\text{Fe}^{\text{II}}-(\text{O}_2)-\text{M}^{3+}$  by electron donors, followed by conversion of  $(14\text{-TMC})\text{Fe}^{\text{II}}-(\text{O}_2)-\text{M}^{3+}$  to  $[(14\text{-TMC})\text{Fe}^{\text{IV}}(\text{O})]^{2+}$  and  $\text{M}^{3+}(\text{O})$  via heterolytic O–O bond cleavage of the peroxide ligand (Scheme 5a).

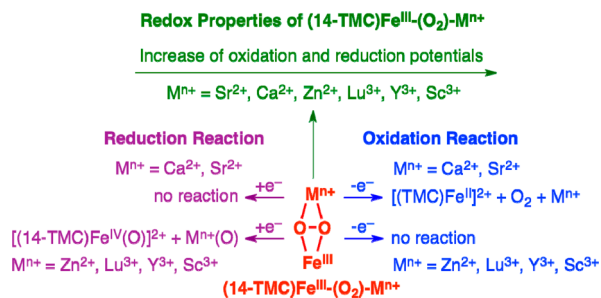
**Scheme 5. Proposed O–O Bond Cleavage Mechanisms of  $(14\text{-TMC})\text{Fe}^{\text{III}}-(\text{O}_2)-\text{M}^{3+}$  (a) and  $(\text{Porp})\text{Fe}^{\text{III}}-(\text{O}_2)-\text{Cu}^{2+}$  (b) in One-Electron Reduction Reactions**



Based on the observation that the redox-inactive metal ions affect the peroxide O–O bond cleavage of the  $\text{Fe}^{\text{III}}\text{-O}_2\text{-M}^{3+}$  moiety, it was proposed that the Cu(II) ion at the active site in cytochrome *c* oxidase (CcO) may function as a Lewis acid that facilitates the one-electron reduction of the Fe(III)-(porphyrin)-O<sub>2</sub>-Cu(II) intermediate to give an Fe(II)-(porphyrin)-O<sub>2</sub>-Cu(II) species, followed by heterolytic O–O bond cleavage of the reduced Fe(II)(porphyrin)-O<sub>2</sub>-Cu(II) species to give the *S* = 1 Fe(IV)-oxo and Cu(II) species (Scheme 5b).<sup>42,43</sup>

Mononuclear nonheme iron(III)-peroxo complexes binding other redox-inactive metal ions, such as  $\text{Sr}^{2+}$ ,  $\text{Ca}^{2+}$ ,  $\text{Zn}^{2+}$ , and  $\text{Lu}^{3+}$ , were synthesized recently and used to investigate the effects of the redox-inactive metal ion on the redox properties and reactivities of  $(14\text{-TMC})\text{Fe}^{\text{III}}-(\text{O}_2)-\text{M}^{n+}$  (Scheme 6).<sup>44</sup>

**Scheme 6. Effects of Redox-Inactive Metal Ions on the Redox Properties and Reduction and Oxidation Reactions of  $(14\text{-TMC})\text{Fe}^{\text{III}}-(\text{O}_2)-\text{M}^{n+}$  Complexes**



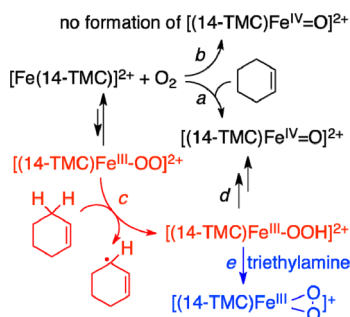
When the redox properties of  $(14\text{-TMC})\text{Fe}^{\text{III}}-(\text{O}_2)-\text{M}^{n+}$  ( $\text{M}^{n+} = \text{Sr}^{2+}$ ,  $\text{Ca}^{2+}$ ,  $\text{Zn}^{2+}$ ,  $\text{Lu}^{3+}$ ,  $\text{Y}^{3+}$ , and  $\text{Sc}^{3+}$ ) were determined using cyclic voltammetry, the one-electron oxidation and reduction potentials of  $(14\text{-TMC})\text{Fe}^{\text{III}}-(\text{O}_2)-\text{M}^{n+}$  varied depending on the Lewis acidity of the redox-inactive metal ions. Both one-electron oxidation and reduction potentials became more positive as the Lewis acidity of  $\text{M}^{n+}$  increased (Scheme 6); that is, one-electron oxidation of  $(14\text{-TMC})\text{Fe}^{\text{III}}-(\text{O}_2)-\text{M}^{n+}$

becomes more favorable with the decrease of the Lewis acidity of  $\text{M}^{n+}$ , whereas one-electron reduction of  $(14\text{-TMC})\text{Fe}^{\text{III}}-(\text{O}_2)-\text{M}^{n+}$  is more favorable with the increase of the Lewis acidity of  $\text{M}^{n+}$ . The effect of the Lewis acidity of the redox-inactive metal ions on the reactivities of  $(14\text{-TMC})\text{Fe}^{\text{III}}-(\text{O}_2)-\text{M}^{n+}$  was then investigated by performing one-electron reduction and oxidation reactions using reductant (e.g., 1-benzyl-1,4-dihydropyridinamide dimer ( $\text{BNA}_2$ )) and oxidant (e.g., ceric ammonium nitrate (CAN)). For example, the  $(14\text{-TMC})\text{Fe}^{\text{III}}-(\text{O}_2)-\text{M}^{n+}$  ( $\text{M}^{n+} = \text{Zn}^{2+}$ ,  $\text{Lu}^{3+}$ ,  $\text{Y}^{3+}$ , and  $\text{Sc}^{3+}$ ) complexes were converted to  $[(14\text{-TMC})\text{Fe}^{\text{IV}}(\text{O})]^{2+}$  in the one-electron reduction reactions, whereas  $(14\text{-TMC})\text{Fe}^{\text{III}}-(\text{O}_2)-\text{M}^{n+}$  ( $\text{M}^{n+} = \text{Ca}^{2+}$  and  $\text{Sr}^{2+}$ ) remained intact without being reduced by the one-electron donor (Scheme 6, reduction reaction). Interestingly, when the electron-transfer oxidation of  $(14\text{-TMC})\text{Fe}^{\text{III}}-(\text{O}_2)-\text{M}^{n+}$  was examined using CAN as an oxidant, the peroxide ligand in  $(14\text{-TMC})\text{Fe}^{\text{III}}-(\text{O}_2)-\text{M}^{n+}$  ( $\text{M}^{n+} = \text{Ca}^{2+}$  and  $\text{Sr}^{2+}$ ) as well as in  $[(14\text{-TMC})\text{Fe}^{\text{III}}(\text{O}_2)]^+$  was released as  $\text{O}_2$  but that in the reactions of  $(14\text{-TMC})\text{Fe}^{\text{III}}-(\text{O}_2)-\text{M}^{n+}$  ( $\text{M}^{n+} = \text{Zn}^{2+}$ ,  $\text{Lu}^{3+}$ ,  $\text{Y}^{3+}$ , and  $\text{Sc}^{3+}$ ) was not (Scheme 6, oxidation reaction). These results were interpreted in terms of the effect of the Lewis acidity of the redox-inactive metal ions on the tuning of the one-electron oxidation potentials of the  $(14\text{-TMC})\text{Fe}^{\text{III}}-(\text{O}_2)-\text{M}^{n+}$  complexes; electron transfer from  $[(14\text{-TMC})\text{Fe}^{\text{III}}(\text{O}_2)]^+$  and  $(14\text{-TMC})\text{Fe}^{\text{III}}-(\text{O}_2)-\text{M}^{n+}$  ( $\text{M}^{n+} = \text{Ca}^{2+}$  and  $\text{Sr}^{2+}$ ) to CAN is thermodynamically feasible, whereas no electron transfer from  $(14\text{-TMC})\text{Fe}^{\text{III}}-(\text{O}_2)-\text{M}^{n+}$  ( $\text{M}^{n+} = \text{Zn}^{2+}$ ,  $\text{Lu}^{3+}$ ,  $\text{Y}^{3+}$ , and  $\text{Sc}^{3+}$ ) to CAN occurs. Thus, it has been concluded that the Lewis acidity of the redox-inactive metal ions is an important factor that controls the one-electron oxidation and reduction potentials of  $(14\text{-TMC})\text{Fe}^{\text{III}}-(\text{O}_2)-\text{M}^{n+}$ , thereby determining the one-electron reduction and oxidation reactions for the O–O bond activation and  $\text{O}_2$ -release processes, respectively. Further, the observation of the  $\text{O}_2$ -release reactivity of  $(14\text{-TMC})\text{Fe}^{\text{III}}-(\text{O}_2)-\text{M}^{n+}$  ( $\text{M}^{n+} = \text{Ca}^{2+}$  and  $\text{Sr}^{2+}$ ) was highlighted due to the mysterious role(s) of  $\text{Ca}^{2+}$  and  $\text{Sr}^{2+}$  ions in water oxidation by the oxygen-evolving complex (OEC) in photosystem II (PSII).<sup>45–47</sup> Although the present results provided strong evidence that the  $\text{Ca}^{2+}$  and  $\text{Sr}^{2+}$  ions do not hinder the  $\text{O}_2$ -release from iron(III)-peroxo species upon one-electron oxidation, the role(s) of  $\text{Ca}^{2+}$  ion in OEC for water oxidation still remains elusive (e.g., the formation of O–O bond, which is the most crucial step in the catalytic cycle of PSII).

## ■ MONONUCLEAR NONHEME IRON(III)–HYDROPEROXO COMPLEXES

Iron(III)-hydroperoxo species (3) are generated upon protonation of iron(III)-peroxo species (2) (Scheme 1, reaction c) or in the reactions of iron(II or III) complexes with  $\text{H}_2\text{O}_2$ .<sup>20,48–50</sup> An alternative method for the generation of iron(III)-hydroperoxo species (3) is a HAA of substrate C–H bonds by iron(III)-superoxo species (1) (Scheme 1, reaction d), which has attracted much attention recently in nonheme iron enzymes and their models.<sup>3,6</sup> Although no direct evidence for the conversion of iron(III)-superoxo to iron(III)-hydroperoxo has been obtained yet, one example supporting the proposed pathway was reported in nonheme iron models, such as the observation of iron(IV)-oxo formation,  $[(14\text{-TMC})\text{Fe}^{\text{IV}}(\text{O})]^{2+}$ , in the activation of  $\text{O}_2$  by an iron(II) complex,  $[\text{Fe}^{\text{II}}(14\text{-TMC})]^{2+}$ , in the presence of olefins (e.g., cyclohexene) (Scheme 7, reaction a).<sup>51</sup> In the absence of the olefinic substrates, no formation of  $[(14\text{-TMC})\text{Fe}^{\text{IV}}(\text{O})]^{2+}$  was

**Scheme 7. Proposed Mechanism for the Conversion of an Iron(III)–Superoxo Species to an Iron(III)–Hydroperoxo Species via H-Atom Abstraction from an Olefinic C–H Bond**



observed (Scheme 7, reaction b). A mechanism was proposed as follows: An iron(III)–hydroperoxo complex,  $[(14\text{-TMC})\text{Fe}^{\text{III}}(\text{O}_2\text{H})]^{2+}$ , was generated by HAA of allylic C–H bonds by a putative iron(III)–superoxo species,  $[(14\text{-TMC})\text{Fe}^{\text{III}}(\text{O}_2)]^{2+}$  (Scheme 7, pathway c), followed by the O–O bond cleavage of the hydroperoxo ligand to form  $[(14\text{-TMC})\text{Fe}^{\text{IV}}(\text{O})]^{2+}$  as the product (Scheme 7, pathway d).<sup>51</sup> Although the key intermediates, such as  $[(14\text{-TMC})\text{Fe}^{\text{III}}(\text{O}_2)]^{2+}$  and  $[(14\text{-TMC})\text{Fe}^{\text{III}}(\text{O}_2\text{H})]^{2+}$ , were not detected in the reaction, indirect evidence for the  $[(14\text{-TMC})\text{Fe}^{\text{III}}(\text{O}_2\text{H})]^{2+}$  species was obtained by trapping an iron(III)–peroxo complex,  $[(14\text{-TMC})\text{Fe}^{\text{III}}(\text{O}_2)]^+$ , when the reaction was carried out in the presence of base (Scheme 7, pathway e).

One of the long-standing controversies in heme and nonheme iron systems is the reactivity of the iron(III)–hydroperoxo species in oxidation reactions, such as sulfoxidation and alkane hydroxylation.<sup>52,53</sup> Although there is a consensus that iron(III)–hydroperoxo species are sluggish oxidants in heme reactions,<sup>53,54</sup> reactivities of nonheme iron(III)–hydroperoxo species are still unclear and are being investigated intensively in experiments and calculations. For example, although synthetic low-spin (LS) iron(III)–hydroperoxo complexes were sluggish oxidants in the oxidation of sulfides, olefins, and aldehydes,<sup>55</sup> a high-spin (HS) iron(III)–hydroperoxo complex,  $[(14\text{-TMC})\text{Fe}^{\text{III}}(\text{O}_2\text{H})]^{2+}$ , showed interesting reactivities in both nucleophilic and electrophilic oxidative reactions.<sup>20</sup> In the nucleophilic oxidative reactions, the iron(III)–hydroperoxo complex was found to be a stronger oxidant than the corresponding iron(III)–peroxo and iron(IV)–oxo complexes in the oxidation of aldehydes. The electrophilic reactivity of the  $[(14\text{-TMC})\text{Fe}^{\text{III}}(\text{O}_2\text{H})]^{2+}$  complex was also investigated in combined experimental and theoretical studies for HAA and OAT reactions.<sup>20,56,57</sup> In HAA reactions, the HS iron(III)–hydroperoxo complex showed a greater reactivity than the LS iron(III)–hydroperoxo complex,  $[(\text{N}4\text{Py})\text{Fe}^{\text{III}}(\text{O}_2\text{H})]^{2+}$  ( $\text{N}4\text{Py} = N,N$ -bis(2-pyridylmethyl)- $N$ -bis(2-pyridyl)methylamine), in the oxidation of alkylaromatic compounds with weak C–H bonds.<sup>56</sup> In OAT reactions, the  $[(14\text{-TMC})\text{Fe}^{\text{III}}(\text{O}_2\text{H})]^{2+}$  complex reacted with sulfides to give the corresponding sulfoxides, and the electrophilic character of the hydroperoxo group in  $[(14\text{-TMC})\text{Fe}^{\text{III}}(\text{O}_2\text{H})]^{2+}$  was demonstrated by showing a Hammett  $\rho$  value of  $-1.1$  in the sulfoxidation of *para*-*X*-thioanisoles.<sup>57</sup> Very recently, a mononuclear nonheme manganese(III)–hydroperoxo complex,  $[(14\text{-TMC})\text{Mn}^{\text{III}}(\text{O}_2\text{H})]^{2+}$ , was synthesized by the protonation of the corresponding manganese(III)–peroxo complex,  $[(14\text{-TMC})\text{Mn}^{\text{III}}(\text{O}_2)]^+$ , and characterized with various spectro-

scopic methods and density functional theory (DFT) calculations.<sup>58</sup> The manganese(III)–hydroperoxo complex was a competent oxidant in OAT reactions, such as the oxidation of sulfides, with a Hammett  $\rho$  value of  $-5.0$  in the sulfoxidation of *para*-*X*-thioanisoles.<sup>58</sup> More detailed mechanistic studies are needed to understand the chemical properties of the newly synthesized manganese(III)–hydroperoxo complex.

Another long-standing debate in the field of heme and nonheme iron enzymatic and biomimetic reactions is the mechanisms of the O–O bond cleavage of the iron(III)–hydroperoxo species (e.g., heterolysis versus homolysis). While the O–O bond cleavage mechanisms have been extensively investigated in heme systems over the past several decades,<sup>1,8,11</sup> such mechanistic studies in nonheme iron(III)–hydroperoxo species have been conducted only recently. For example, it has been shown that the protonation of  $[(14\text{-TMC})\text{Fe}^{\text{III}}(\text{O}_2)]^+$  afforded the formation of  $[(14\text{-TMC})\text{Fe}^{\text{III}}(\text{O}_2\text{H})]^{2+}$ , followed by the hydroperoxo O–O bond cleavage of the latter species to give the  $[(14\text{-TMC})\text{Fe}^{\text{IV}}(\text{O})]^{2+}$  complex.<sup>20,59</sup> Two different mechanisms were proposed for the O–O bond cleavage step: One is O–O bond homolysis to give  $[(14\text{-TMC})\text{Fe}^{\text{IV}}(\text{O})]^{2+}$  and hydroxyl radical (Scheme 1, reaction f).<sup>20</sup> The other possibility is heterolytic hydroperoxo O–O bond cleavage that leads to the generation of  $[(14\text{-TMC})\text{Fe}^{\text{V}}(\text{O})]^{3+}$  (Scheme 1, reaction e), followed by one-electron reduction of the Fe(V)–oxo species to give the  $[(14\text{-TMC})\text{Fe}^{\text{IV}}(\text{O})]^{2+}$  complex (Scheme 1, reaction i).<sup>59</sup> From results of mechanistic studies such as the effects of proton concentration and substrates on the formation of  $[(14\text{-TMC})\text{Fe}^{\text{IV}}(\text{O})]^{2+}$ , it was proposed that HS iron(III)–hydroperoxo species undergoes O–O bond homolysis for the formation of  $[(14\text{-TMC})\text{Fe}^{\text{IV}}(\text{O})]^{2+}$ .<sup>20</sup> More recently, it was shown that one-electron reduction of  $[(14\text{-TMC})\text{Fe}^{\text{III}}(\text{O}_2\text{H})]^{2+}$  by Fc derivatives resulted in the formation of  $[(14\text{-TMC})\text{Fe}^{\text{IV}}(\text{O})]^{2+}$ .<sup>60</sup> Based on the observations that the conversion rates were dependent on the concentration and oxidation potentials of the electron donors, the reduction of the iron(III)–hydroperoxo complex to the one-electron reduced iron(II)–hydroperoxo species,  $[(14\text{-TMC})\text{Fe}^{\text{II}}(\text{O}_2\text{H})]^+$ , was proposed to be the rate-determining step (Scheme 1, reaction g), followed by the heterolytic O–O bond cleavage of the putative iron(II)–hydroperoxo species to give the iron(IV)–oxo complex (Scheme 1, reaction h). A similar conclusion was reached in the mechanistic studies of the O–O bond cleavage of a HS iron(III)–alkylperoxo complex,  $[(13\text{-TMC})\text{Fe}^{\text{III}}(\text{O}_2\text{CR}_3)]^{2+}$ , as a biomimetic model of pterin-dependent hydroxylases,<sup>10</sup> in which one-electron reduction of the iron(III)–alkylperoxo complex afforded formation of an iron(IV)–oxo complex via the O–O bond heterolysis of a reduced iron(II)–alkylperoxo species.<sup>60</sup>

## ■ MONONUCLEAR NONHEME IRON(IV)–OXO COMPLEXES

Since the first X-ray crystal structure of a synthetic mononuclear nonheme iron(IV)–oxo complex,  $[(14\text{-TMC})\text{Fe}^{\text{IV}}(\text{O})]^{2+}$ , was reported in 2003,<sup>16</sup> more than 60 iron(IV)–oxo complexes bearing non-porphyrinic supporting ligands have been synthesized and characterized spectroscopically or structurally, and their reactivities have been intensively investigated in various oxidation reactions as well as in the reactions of electron and hydride transfer, intermolecular oxygen atom transfer, and oxygen atom exchange with water.<sup>6,11–13,15,18</sup> The effects of supporting and axial ligands,

geometry and topology, redox-inactive metal ions and protons, and iron(IV) spin states have also been addressed in the reactivity studies of the synthetic mononuclear nonheme iron(IV)–oxo complexes.<sup>11,15</sup> In addition, theoretical studies using DFT calculations have provided fruitful information on elucidating reaction mechanisms, including transition state structures and reaction pathways, and reactivities of nonheme iron(IV)–oxo complexes.<sup>61,62</sup> Thus, our understanding of the mononuclear nonheme iron(IV)–oxo complexes has been greatly advanced over the past 12 years and is even more advanced than that of the heme analogues. However, there are still some issues that remain elusive, such as the effect of spin states of HS ( $S = 2$ ) and LS ( $S = 1$ ) iron(IV)–oxo complexes<sup>63</sup> and the effect of oxidation states of iron(IV)– and iron(V)–oxo complexes in oxidation reactions. For example, why do mononuclear nonheme iron enzymes use HS iron(IV)–oxo species for their reactions?<sup>61,62</sup> In addition, recent mechanistic studies on the C–H bond activation of alkanes and the oxidation of cyclohexene by nonheme iron(IV)–oxo complexes revealed that there is a significant ligand effect (i.e., heme versus nonheme) that controls the reaction pathways, such as the oxygen rebound versus oxygen non-rebound mechanisms in the C–H bond activation of alkanes and the C=C epoxidation versus allylic C–H bond activation in the cyclohexene oxidation by heme and nonheme iron–oxo complexes, respectively.<sup>64–66</sup> Due to the brevity of this Account, readers may refer to the excellent reviews published recently on the generation, structural and spectroscopic characterization, and reactivity studies of synthetic mononuclear nonheme iron(IV)–oxo complexes for detailed information.<sup>6,11–13,15,17–19</sup>

## SUMMARY

In this Account, we have demonstrated that biomimetic studies using simple synthetic metal complexes have advanced our understanding of the chemical and physical properties of the thermally unstable and highly reactive metal–oxygen intermediates involved in the catalytic cycles of dioxygen activation by metalloenzymes. Indeed, a tremendous amount of work has been accomplished over the past decade on the synthesis, characterization, and reactivity studies of biomimetic iron–oxygen intermediates. Despite the great advances in understanding many aspects of mononuclear nonheme iron–oxygen intermediates, continued extensive research is needed to fully elucidate the chemical properties of the biologically important iron–oxygen species, including the currently less understood iron(III)–superoxo species.

## AUTHOR INFORMATION

### Corresponding Author

\*E-mail: [wwnam@ewha.ac.kr](mailto:wwnam@ewha.ac.kr).

### Notes

The authors declare no competing financial interest.

### Biography

**Wonwoo Nam** received his B.S. (Honors) degree in Chemistry from California State University, Los Angeles, and his Ph.D. degree in Inorganic Chemistry from UCLA under the direction of Professor Joan S. Valentine in 1990. After one year postdoctoral experience at UCLA, he became an Assistant Professor at Hong Ik University in 1991. He moved to Ewha Womans University in 1994, where he is currently a Distinguished Professor of Ewha Womans University.

## ACKNOWLEDGMENTS

I thank the past and present students, postdoctoral fellows, and collaborators whose names appear in the list of references. Financial support from the NRF of Korea through CRI (Grant NRF-2012R1A3A2048842) and GRL (Grant NRF-2010-00353) is greatly acknowledged. This Account is dedicated to Professor Joan S. Valentine at Ewha Womans University on her 70th birthday.

## REFERENCES

- (1) Nam, W. Dioxygen activation by metalloenzymes and models. *Acc. Chem. Res.* **2007**, *40*, 465 and articles in the special issue. DOI: 10.1021/ar700131d.
- (2) Holm, R. H.; Solomon, E. I. Introduction: Bioinorganic enzymology II. *Chem. Rev.* **2014**, *114*, 3367–3368 and reviews in the special issue. DOI: 10.1021/cr500118g.
- (3) van der Donk, W. A.; Krebs, C.; Bollinger, J. M., Jr. Substrate activation by iron superoxo intermediates. *Curr. Opin. Struct. Biol.* **2010**, *20*, 673–683.
- (4) Kovaleva, E. G.; Lipscomb, J. D. Versatility of biological non-heme Fe(II) centers in oxygen activation reactions. *Nat. Chem. Biol.* **2008**, *4*, 186–193.
- (5) Krebs, C.; Fujimori, D. G.; Walsh, C. T.; Bollinger, J. M., Jr. Non-heme Fe(IV)-oxo intermediates. *Acc. Chem. Res.* **2007**, *40*, 484–492.
- (6) Ray, K.; Pfaff, F. F.; Wang, B.; Nam, W. Status of reactive non-heme metal-oxygen intermediates in chemical and enzymatic reactions. *J. Am. Chem. Soc.* **2014**, *136*, 13942–13958.
- (7) Solomon, E. I.; Light, K. M.; Liu, L. V.; Srncic, M.; Wong, S. D. Geometric and electronic structure contributions to function in non-heme iron enzymes. *Acc. Chem. Res.* **2013**, *46*, 2725–2739.
- (8) Ortiz de Montellano, P. R. Hydrocarbon hydroxylation by cytochrome P450 enzymes. *Chem. Rev.* **2010**, *110*, 932–948.
- (9) Baldwin, J. E.; Bradley, M. Isopenicillin N synthase: Mechanistic studies. *Chem. Rev.* **1990**, *90*, 1079–1088.
- (10) Abu-Omar, M. M.; Loaiza, A.; Hontzeas, N. Reaction mechanisms of mononuclear non-heme iron oxygenases. *Chem. Rev.* **2005**, *105*, 2227–2252.
- (11) Nam, W. High-valent iron(IV)-oxo complexes of heme and non-heme ligands in oxygenation reactions. *Acc. Chem. Res.* **2007**, *40*, 522–531.
- (12) Que, L., Jr. The road to non-heme oxoferryls and beyond. *Acc. Chem. Res.* **2007**, *40*, 493–500.
- (13) Hohenberger, J.; Ray, K.; Meyer, K. The biology and chemistry of high-valent iron-oxo and iron-nitrido complexes. *Nat. Commun.* **2012**, *3*, 720.
- (14) Cho, J.; Sarangi, R.; Nam, W. Mononuclear metal-O<sub>2</sub> complexes bearing macrocyclic N-tetramethylated cyclam ligands. *Acc. Chem. Res.* **2012**, *45*, 1321–1330.
- (15) Nam, W.; Lee, Y.-M.; Fukuzumi, S. Tuning reactivity and mechanism in oxidation reactions by mononuclear nonheme iron(IV)-oxo complexes. *Acc. Chem. Res.* **2014**, *47*, 1146–1154.
- (16) Rohde, J.-U.; In, J.-H.; Lim, M. H.; Brennessel, W. W.; Bukowski, M. R.; Stubna, A.; Münck, E.; Nam, W.; Que, L., Jr. Crystallographic and spectroscopic characterization of a nonheme Fe(IV)=O complex. *Science* **2003**, *299*, 1037–1039.
- (17) Fukuzumi, S. Electron-transfer properties of high-valent metal-oxo complexes. *Coord. Chem. Rev.* **2013**, *257*, 1564–1575.
- (18) de Visser, S. P.; Rohde, J.-U.; Lee, Y.-M.; Cho, J.; Nam, W. Intrinsic properties and reactivities of mononuclear nonheme iron-oxygen complexes bearing the tetramethylcyclam ligand. *Coord. Chem. Rev.* **2013**, *257*, 381–393.
- (19) Ray, K.; Heims, F.; Schwalbe, M.; Nam, W. High-valent metal-oxo intermediates in energy demanding processes: from dioxygen reduction to water splitting. *Curr. Opin. Chem. Biol.* **2015**, *25*, 159–171.
- (20) Cho, J.; Jeon, S.; Wilson, S. A.; Liu, L. V.; Kang, E. A.; Braymer, J. J.; Lim, M. H.; Hedman, B.; Hodgson, K. O.; Valentine, J. S.;

Solomon, E. I.; Nam, W. Structure and reactivity of a mononuclear non-haem iron(III)-peroxo complex. *Nature* **2011**, *478*, 502–505.

(21) Hong, S.; Sutherland, K. D.; Park, J.; Kwon, E.; Siegler, M. A.; Solomon, E. I.; Nam, W. Crystallographic and spectroscopic characterization and reactivities of a mononuclear non-haem iron(III)-superoxo complex. *Nat. Commun.* **2014**, *5*, 5440.

(22) de Visser, S. P. Elucidating enzyme mechanism and intrinsic chemical properties of short-lived intermediates in the catalytic cycles of cysteine dioxygenase and taurine/ $\alpha$ -ketoglutarate dioxygenase. *Coord. Chem. Rev.* **2009**, *253*, 754–768.

(23) Phillips, S. E. V. Structure of oxymyoglobin. *Nature* **1978**, *273*, 247–248.

(24) Collman, J. P.; Gagne, R. R.; Reed, C. A.; Robinson, W. T.; Rodley, G. A. Structure of an iron(II) dioxygen complex; a model for oxygen carrying hemoproteins. *Proc. Natl. Acad. Sci. U. S. A.* **1974**, *71*, 1326–1329.

(25) Chiang, C.-W.; Kleespies, S. T.; Stout, H. D.; Meier, K. K.; Li, P.-Y.; Bominaar, E. L.; Que, L., Jr.; Münck, E.; Lee, W.-Z. Characterization of a paramagnetic mononuclear nonheme iron-superoxo complex. *J. Am. Chem. Soc.* **2014**, *136*, 10846–10849.

(26) Kovaleva, E. G.; Lipscomb, J. D. Crystal structures of Fe<sup>2+</sup> dioxygenase superoxo, alkylperoxo, and bound product intermediates. *Science* **2007**, *316*, 453–457.

(27) Cramer, C. J.; Tolman, W. B.; Theopold, K. H.; Rheingold, A. L. Variable character of O–O and M–O bonding in side-on ( $\eta^2$ ) 1:1 metal complexes of O<sub>2</sub>. *Proc. Natl. Acad. Sci. U. S. A.* **2003**, *100*, 3635–3640.

(28) Pirovano, P.; Magherusan, A. M.; McGlynn, C.; Ure, A.; Lynes, A.; McDonald, A. R. Nucleophilic reactivity of a copper(II)-superoxide complex. *Angew. Chem., Int. Ed.* **2014**, *53*, 5946–5950.

(29) Himes, R. A.; Karlin, K. D. Copper–dioxygen complex mediated C–H bond oxygenation: Relevance for particulate methane monooxygenase (pMMO). *Curr. Opin. Chem. Biol.* **2009**, *13*, 119–131.

(30) Yao, S.; Driess, M. Lessons from isolable nickel(I) precursor complexes for small molecule activation. *Acc. Chem. Res.* **2012**, *45*, 276–287.

(31) Cho, J.; Woo, J.; Nam, W. An “end-on” chromium(III)-superoxo complex: Crystallographic and spectroscopic characterization and reactivity in C–H bond activation of hydrocarbons. *J. Am. Chem. Soc.* **2010**, *132*, 5958–5959.

(32) Cho, J.; Woo, J.; Nam, W. A chromium(III)-superoxo complex in oxygen atom transfer reactions as a chemical model of cysteine dioxygenase. *J. Am. Chem. Soc.* **2012**, *134*, 11112–11115.

(33) Sastri, C. V.; Park, M. J.; Ohta, T.; Jackson, T. A.; Stubna, A.; Seo, M. S.; Lee, J.; Kim, J.; Kitagawa, T.; Münck, E.; Que, L., Jr.; Nam, W. Axial ligand substituted nonheme Fe<sup>IV</sup>=O complexes: Observation of near-UV LMCT bands and Fe=O Raman vibrations. *J. Am. Chem. Soc.* **2005**, *127*, 12494–12495.

(34) Yokoyama, A.; Cho, K.-B.; Karlin, K. D.; Nam, W. Reactions of a chromium(III)-superoxo complex and nitric oxide that lead to the formation of chromium(IV)-oxo and chromium(III)-nitrito complexes. *J. Am. Chem. Soc.* **2013**, *135*, 14900–14903.

(35) Wertz, D. L.; Valentine, J. S. Nucleophilicity of iron-peroxo porphyrin complexes. *Struct. Bonding (Berlin)* **2000**, *97*, 37–60.

(36) Karlsson, A.; Parales, J. V.; Parales, R. E.; Gibson, D. T.; Eklund, H.; Ramaswamy, S. Crystal structure of naphthalene dioxygenase: Side-on binding of dioxygen to iron. *Science* **2003**, *299*, 1039–1042.

(37) Yokoyama, A.; Han, J. E.; Cho, J.; Kubo, M.; Ogura, T.; Siegler, M. A.; Karlin, K. D.; Nam, W. Chromium(IV)-peroxo complex formation and its nitric oxide dioxygenase reactivity. *J. Am. Chem. Soc.* **2012**, *134*, 15269–15272.

(38) Kang, H.; Cho, J.; Cho, K.-B.; Nomura, T.; Ogura, T.; Nam, W. Mononuclear manganese-peroxo and bis( $\mu$ -oxo)dimanganese complexes bearing a common N-methylated macrocyclic ligand. *Chem. - Eur. J.* **2013**, *19*, 14119–14125.

(39) Cho, J.; Kang, H. Y.; Liu, L. V.; Sarangi, R.; Solomon, E. I.; Nam, W. Mononuclear nickel(II)-superoxo and nickel(III)-peroxo complexes bearing a common macrocyclic TMC ligand. *Chem. Sci.* **2013**, *4*, 1502–1508.

(40) Lee, Y.-M.; Bang, S.; Kim, Y. M.; Cho, J.; Hong, S.; Nomura, T.; Ogura, T.; Troeppner, O.; Ivanović-Burmazović, I.; Sarangi, R.; Fukuzumi, S.; Nam, W. A mononuclear nonheme iron(III)-peroxo complex binding redox-inactive metal ions. *Chem. Sci.* **2013**, *4*, 3917–3923.

(41) Li, F.; Van Heuvelen, K. M.; Meier, K. K.; Münck, E.; Que, L., Jr. Sc<sup>3+</sup>-triggered oxoiron(IV) formation from O<sub>2</sub> and its non-heme iron(II) precursor via a Sc<sup>3+</sup>-peroxo-Fe<sup>3+</sup> intermediate. *J. Am. Chem. Soc.* **2013**, *135*, 10198–10201.

(42) Chufán, E. E.; Puiu, S. C.; Karlin, K. D. Heme–copper/dioxygen adduct formation, properties, and reactivity. *Acc. Chem. Res.* **2007**, *40*, 563–572.

(43) Kaila, V. R. I.; Verkhovsky, M. I.; Wikström, M. Proton-coupled electron transfer in cytochrome oxidase. *Chem. Rev.* **2010**, *110*, 7062–7081.

(44) Bang, S.; Lee, Y.-M.; Hong, S.; Cho, K.-B.; Nishida, Y.; Seo, M. S.; Sarangi, R.; Fukuzumi, S.; Nam, W. Redox-inactive metal ions modulate the reactivity and oxygen release of mononuclear non-haem iron(III)-peroxo complexes. *Nat. Chem.* **2014**, *6*, 934–940.

(45) Lionetti, D.; Agapie, T. How calcium affects oxygen formation. *Nature* **2014**, *513*, 495–496.

(46) Suga, M.; Akita, F.; Hirata, K.; Ueno, G.; Murakami, H.; Nakajima, Y.; Shimizu, T.; Yamashita, K.; Yamamoto, M.; Ago, H.; Shen, J.-R. Native structure of photosystem II at 1.95 Å resolution viewed by femtosecond X-ray pulses. *Nature* **2015**, *517*, 99–103.

(47) Rivalta, I.; Brudvig, G. W.; Batista, V. S. Oxomanganese complexes for natural and artificial photosynthesis. *Curr. Opin. Chem. Biol.* **2012**, *16*, 11–18.

(48) Jensen, K. B.; McKenzie, C. J.; Nielsen, L. P.; Pedersen, J. Z.; Svendsen, H. M. Deprotonation of low-spin mononuclear iron(III)-hydroperoxide complexes give transient blue species assigned to high-spin iron(III)-peroxide complexes. *Chem. Commun.* **1999**, 1313–1314.

(49) Wada, A.; Ogo, S.; Nagatomo, S.; Kitagawa, T.; Watanabe, Y.; Jitsukawa, K.; Masuda, H. Reactivity of hydroperoxide bound to a mononuclear non-heme iron site. *Inorg. Chem.* **2002**, *41*, 616–618.

(50) Bukowski, M. R.; Comba, P.; Limberg, C.; Merz, M.; Que, L., Jr.; Wistuba, T. Bispidine ligand effects on iron/hydrogen peroxide chemistry. *Angew. Chem., Int. Ed.* **2004**, *43*, 1283–1287.

(51) Lee, Y.-M.; Hong, S.; Morimoto, Y.; Shin, W.; Fukuzumi, S.; Nam, W. Dioxygen activation by a non-heme iron(II) complex: Formation of an iron(IV)-oxo complex via C–H activation by a putative iron(III)-superoxo species. *J. Am. Chem. Soc.* **2010**, *132*, 10668–10670.

(52) Nam, W.; Ryu, Y. O.; Song, W. J. Oxidizing intermediates in cytochrome P450 model reactions. *JBIC, J. Biol. Inorg. Chem.* **2004**, *9*, 654–660.

(53) Shaik, S.; de Visser, S. P.; Kumar, D. One oxidant, many pathways: a theoretical perspective of monooxygenation mechanisms by cytochrome P450 enzymes. *JBIC, J. Biol. Inorg. Chem.* **2004**, *9*, 661–668.

(54) Wang, B.; Li, C.; Cho, K.-B.; Nam, W.; Shaik, S. The Fe<sup>III</sup>(H<sub>2</sub>O<sub>2</sub>) complex as a highly efficient oxidant in sulfoxidation reactions: Revival of an underrated oxidant in cytochrome P450. *J. Chem. Theory Comput.* **2013**, *9*, 2519–2525.

(55) Park, M. J.; Lee, J.; Suh, Y.; Kim, J.; Nam, W. Reactivities of mononuclear non-heme iron intermediates including evidence that iron(III)-hydroperoxo species is a sluggish oxidant. *J. Am. Chem. Soc.* **2006**, *128*, 2630–2634.

(56) Liu, L. V.; Hong, S.; Cho, J.; Nam, W.; Solomon, E. I. Comparison of high-spin and low-spin nonheme Fe<sup>III</sup>-OOH complexes in O–O bond homolysis and H-atom abstraction reactions. *J. Am. Chem. Soc.* **2013**, *135*, 3286–3299.

(57) Kim, Y. M.; Cho, K.-B.; Cho, J.; Wang, B.; Li, C.; Shaik, S.; Nam, W. A mononuclear non-heme high-spin iron(III)-hydroperoxo complex as an active oxidant in sulfoxidation reactions. *J. Am. Chem. Soc.* **2013**, *135*, 8838–8841.

(58) So, H.; Park, Y. J.; Cho, K.-B.; Lee, Y.-M.; Seo, M. S.; Cho, J.; Sarangi, R.; Nam, W. Spectroscopic characterization and reactivity



studies of a mononuclear nonheme Mn(III)-hydroperoxo complex. *J. Am. Chem. Soc.* **2014**, *136*, 12229–12232.

(59) Li, F.; Meier, K. K.; Cranswick, M. A.; Chakrabarti, M.; Van Heuvelen, K. M.; Münck, E.; Que, L., Jr. Characterization of a high-spin non-heme Fe<sup>III</sup>-OOH intermediate and its quantitative conversion to an Fe<sup>IV</sup>=O complex. *J. Am. Chem. Soc.* **2011**, *133*, 7256–7259.

(60) Bang, S.; Park, S.; Lee, Y.-M.; Hong, S.; Cho, K.-B.; Nam, W. Demonstration of heterolytic O-O bond cleavage of putative nonheme iron(II)-OOH(R) complexes for Fenton and enzymatic reactions. *Angew. Chem., Int. Ed.* **2014**, *53*, 7843–7847.

(61) Shaik, S.; Chen, H.; Janardanan, D. Exchange-enhanced reactivity in bond activation by metal-oxo enzymes and synthetic reagents. *Nat. Chem.* **2011**, *3*, 19–27.

(62) Usharani, D.; Janardanan, D.; Li, C.; Shaik, S. A theory for bioinorganic chemical reactivity of oxometal complexes and analogous oxidants: The exchange and orbital-selection rules. *Acc. Chem. Res.* **2013**, *46*, 471–482.

(63) Biswas, A. N.; Puri, M.; Meier, K. K.; Oloo, W. N.; Rohde, G. T.; Bominaar, E. L.; Münck, E.; Que, L., Jr. Modeling TauD-J: A high-spin nonheme oxoiron(IV) complex with high reactivity toward C-H bonds. *J. Am. Chem. Soc.* **2015**, *137*, 2428–2431.

(64) Cho, K.-B.; Wu, X.; Lee, Y.-M.; Kwon, Y. H.; Shaik, S.; Nam, W. Evidence for an alternative to the oxygen rebound mechanism in C-H bond activation by nonheme Fe<sup>IV</sup>O complexes. *J. Am. Chem. Soc.* **2012**, *134*, 20222–20225.

(65) Kwon, Y. H.; Mai, B. K.; Lee, Y.-M.; Dhuri, S. N.; Mandal, D.; Cho, K.-B.; Kim, Y.; Shaik, S.; Nam, W. Determination of spin inversion probability, H-tunneling correction, and regioselectivity in the two-state reactivity of nonheme iron(IV)-oxo complexes. *J. Phys. Chem. Lett.* **2015**, *6*, 1472–1476.

(66) Dhuri, S. N.; Cho, K.-B.; Lee, Y.-M.; Shin, S. Y.; Kim, J. H.; Mandal, D.; Shaik, S.; Nam, W. Interplay of experiment and theory in elucidating mechanisms of oxidation reactions by a nonheme Ru<sup>IV</sup>O complex. *J. Am. Chem. Soc.* **2015**, *137*, 8623–8632.